Computational Materials Science 141 (2018) 75–81

Contents lists available at ScienceDirect

Computational Materials Science

journal homepage: www.elsevier.com/locate/commatsci

Evaluation of point-core approximation effect on the positron energy levels in diamond structure solids

Jie Zhang [a,*], Shaojuan Fan [b], Jiandang Liu [c], Changle Liu [a], Bangjiao Ye [c], Xiang Gao [a,c], Damao Yao [a,c]

[a] Institute of Plasma Physics, Chinese Academy of Sciences, Hefei 230031, China
[b] Hefei Guoxuan High-Technology Power Energy Limited Company, Hefei 230011, China
[c] University of Science and Technology of China, Hefei 230026, China

ARTICLE INFO

Article history:
Received 11 April 2017
Received in revised form 6 September 2017
Accepted 7 September 2017

Keywords:
Point-core approximation
Positron-related parameters
Norm-conserving pseudopotential

ABSTRACT

Positron work function, positron affinity, positron energy band, deformation potential and some other important positron-related parameters are studied in the elemental semiconductors which have the diamond structure, using the first-principle norm-conserving pseudopotential method. While both the local density approximation (LDA) and the generalized gradient approximation (GGA) are employed in the positron structure theoretical research, to deal with the positron-electron exchange-correlation (EC) energy, only the GGA framework is adopted in electron total energy calculation. The nonlinear core correction is included in the positron-electron EC potential and the core electrons are considered within the frozen-core model. Point-core approximation is used to model the positron-ion interact potential. The calculation results agree well with the reference data. However, the positron band effective mass which has a dominate part of the total effective mass is systematic lower than the result which is obtained from other approaches. Because of the sensibility of the positron diffusion constant to the total effective mass, it is found that the point-core approximation could not provide an accurate forecast for the diffusion parameter.

1. Introduction

Many experimental methods based on positron annihilation have been applied to material science since it had been discovered in the last century. They give much valuable information on the electronic structures of condensed media, especially defects in solids [1,2], and belong to one of the few methods which could detect the electron Fermi surfaces directly [3,4]. These positron related experimental results are usually, however, complicated in the form of the positron or data related to the momentum content of the annihilating electron-positron pair in a specific environment. So, the interpretation of these data calls for theoretical methods with quantitative predicting power [5]. Much as in the case of other methods, the theory of positron annihilation has developed from some models which describes the positron-solid interaction to "first-principle" methods predicting the annihilation characteristics for different environments and conditions [6], each method has unique features. One of the most popular first-principle methods is the pseudopotential framework, because that it can be used to treat large defect systems without miss much precision under the present computing conditions, and therefore it is used in this paper to study the positron levels and related parameters.

Although it is well known that surface effect is complicate, the positron affinity, which is defined as the sum of the positron and electron chemical potential, is independent of the surface properties. That is to say, the standard first-principle methods can be used to calculate it. This positron parameter can be understood generally in two different physical pictures. The first one is that it can be defined as the energy gained by taking a thermalized positron from the vacuum level to the lowest bulk energy level [7,8]. The other definition which is first established in metals by Puska et al. [9] is related to the Fermi level in two different conductors. In this picture, the positron affinity is often labeled as A_+ ($A_+ = \mu_- + mu_+$, μ_- and μ_+ represent the electron and positron chemical potential respectively), and is much more widely used in positron related calculation. In this paper, the second definition is also used. The positron work function is expressed as $\varphi_+ = -\varphi_- - A_+$, where φ_- and φ_+ represent the electron and positron work function respectively. In this definition, the electron work function is the vacuum energy level minus the Fermi energy level.

The positrons may experience many processes such as thermalization, diffusion, trapping and so on after they implanted into a

* Corresponding author.
E-mail address: jzhang@ipp.ac.cn (J. Zhang).

http://dx.doi.org/10.1016/j.commatsci.2017.09.017
0927-0256/

solid. In the thermalization process, when positron energy is lower than ~1 eV, interaction between positron and longitudinal acoustic phonons becomes much more important than the inelastic scattering effect in solids, and this gives rise to the longer positron lifetime especially at low temperature. So, the deformation potential theory which is used to theoretical research the positron-phonon interaction plays an important role in the low temperature positron lifetime spectroscopy experiment. In this theory scheme, the positron diffusion constant mainly concerns with the positron effective mass and the deformation potential at a temperature. As a consequence, the two parameters are calculated.

During the past decades, due to the convenient of selecting the so-called crystal zero, many researchers focused on the linear muffin tin orbital approach within the atomic sphere approximation (LMTO-ASA) when they studied the positron energy level [9–12]. In the year about 1999, Panda et al. gave a reliable result within the first-principle norm-conserving pseudopotential (NCPP) framework [8]. After that, few researchers focus on it in the field of positron energy level research, and hence, it is needed to prove the reliability of this approach further. In the present work, this method is used to study the positron affinity. To move forward a single step, the other related parameters such as positron effective mass, work function et al. are obtained.

Here, the elemental semiconductors diamond (C), silicon (Si) and germanium (Ge) are taken as examples. The paper is organized as follows: in Section 2, the calculation model and theoretical background are briefly introduced. Section 3 gives the calculation results and some discussions. At last, it is concluded in Section 4.

2. Calculation model and method

All of C, Si and Ge belong to space group of Fd3m, each primitive cell has two atoms. The input lattice constants for geometry optimization of them are 3.58 Å, 5.43 Å and 5.66 Å respectively [8,13]. Since the LDA and GGA corrections for electron energy level calculations are not very important in positron related parameters computations [8], only the GGA in the scheme of Perdew-Burke-Ernzerhof (PBE) is used at the present work for correcting the electron-electron exchange–correlation (XC) potential [14,15]. The pseudo atomic calculation is performed for C $2s^2 2p^2$, Si $3s^2 3p^2$ and Ge $4s^2 4p^2$. The electronic wave functions are expanded in a plane wave basis set with energy cut off 680 eV for C, 350 eV for Si and 400 eV for Ge. The $8 \times 8 \times 8$, $6 \times 6 \times 6$ and $4 \times 4 \times 4$ Monkhorst-Pack meshes are used to sample the Brillouin zones of C, Si and Ge respectively. The convergence tolerance of maximum energy change, the maximum force, the maximum stress and the maximum displacement for all the researched semiconductors are set to 1.0×10^{-5} eV/atom, 0.03 eV/Å, 0.05 GPa, 0.001 Å, respectively. In the electron work function calculation, the self-consistent dipole correction which was supposed by Neugebauer and Scheffler is considered [16].

In positronic structure calculation, the nonlinear core correction (NLCC) is included to manage the positron-electron XC energy and the core electrons are deal within the frozen-core approximation, which assumes that the core electrons are not polarized by the positron. Louie et al. have shown that the addition of a pseudocore electron density to the pseudovalence electron density gives accurate estimation of the XC potential [17,18]. The point-core approximation (PCA) model is used to construct the positron-ion coulomb interaction potential, and it has been used in the positron annihilation calculation within the pseudopotential framework [19–21]. However, the PCA effect on the positron energy level structure has not been researched systematically. Therefore, there are mainly two purposes to write this paper, one is to further prove the reliability of the NCPP in the field of positron level calculation, and the other is to evaluate the PCA effect on the positron level in solids.

The positronic wavefunctions are usually expanded in the plane wave basis set:

$$\Psi_{nk} = \frac{1}{\sqrt{\Omega}} \sum_{\boldsymbol{K}} C_{nk} \cdot exp(i(\boldsymbol{k} + \boldsymbol{K}) \cdot \boldsymbol{r}) \tag{1}$$

and the positronic schrodinger equation can be written as (in Hartree atomic units):

$$\sum_{\boldsymbol{K}} [A \cdot \delta_{\boldsymbol{K}\boldsymbol{K}'} + V_t(\boldsymbol{G})] \cdot C_{nk}(\boldsymbol{K}) = 0 \tag{2}$$

Table 1
Optimized structural data, and the electron work functions of three different surfaces for C, Si and Ge. The unit of work function is eV.

Host	a_0 (Å)	ε_∞	Electron work function (eV)		
			[1 0 0]	[1 1 0]	[1 1 1]
C	3.579	5.62	6.81	4.96	4.08 3.50 [31]
Si	5.478	11.90	5.13 4.91 [32]	4.47	4.74 4.74 [32]
Ge	5.783	16.00	4.98	4.67	4.63 4.80 [32]

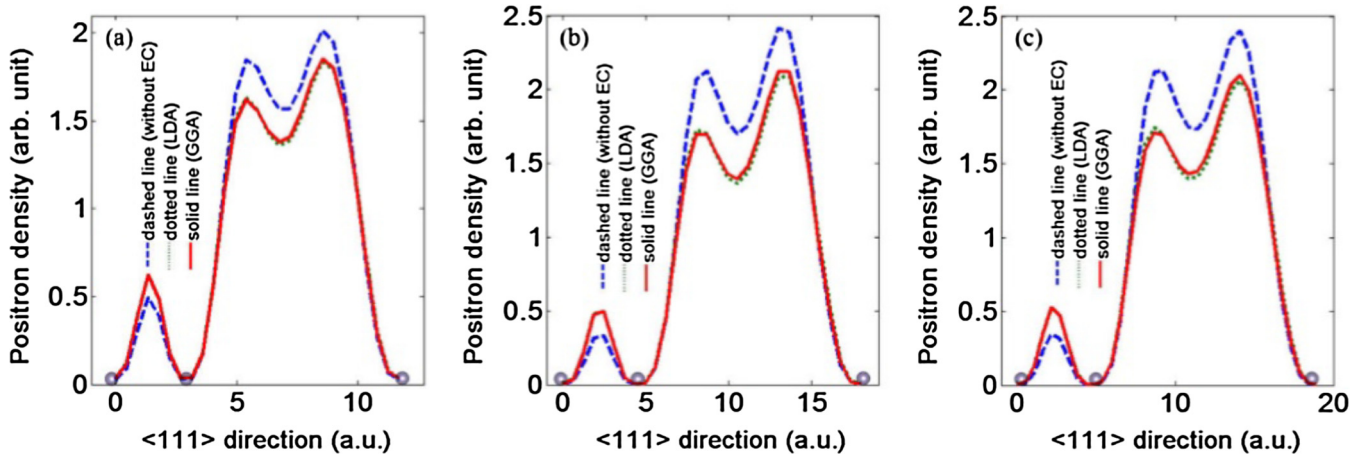

Fig. 1. The thermalized positron density distribution in the unit cell along the ⟨1 1 1⟩ direction within different positron-electron EC potential, the dashed lines represent without the EC effect, the dotted lines and the solid lines express the LDA and GGA schemes respectively, and (a) for C, (b) for Si and (c) for Ge.

where $\boldsymbol{G} = \boldsymbol{K} - \boldsymbol{K}'$, $A = 0.5 \cdot (\boldsymbol{k} + \boldsymbol{K})^2 - E_n(\boldsymbol{k})$, $\boldsymbol{K}$ is reciprocal vector of the crystal, $\boldsymbol{k}$ is positron wave vector and $V_t(\boldsymbol{G})$ is the total potential sensed by the positron in the reciprocal space:

$$V_t(\boldsymbol{G}) = V_{ion}(\boldsymbol{G}) + V_H(\boldsymbol{G}) + V_{xc}(\boldsymbol{G}) \tag{3}$$

$$V_{ion}(\boldsymbol{G}) = \frac{4\pi}{\Omega}\sum_{\alpha}\frac{Z_\alpha}{G^2}\cdot \exp(i\mathbf{G}\cdot\tau_\alpha) \tag{4}$$

$$V_H(\boldsymbol{G}) = \frac{-4\pi}{\Omega G^2}\cdot\int \rho(\boldsymbol{r}')\cdot\exp(i\boldsymbol{G}\cdot\boldsymbol{r}')d\boldsymbol{r}' \tag{5}$$

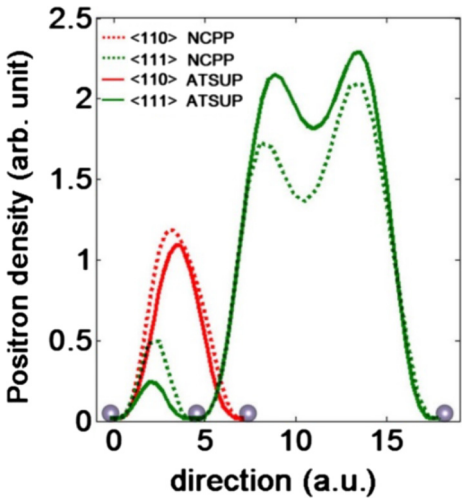

Fig. 2. The positron density distributions of Si in the ⟨1 1 0⟩ and ⟨1 1 1⟩ directions. The solid lines are the ATSUP results and the dotted are the NCPP results. LDA scheme is adopted to handle the positron-electron EC potential in the two methods.

where $V_{xc}(\boldsymbol{G})$ is the Fourier transform of the positron-electron XC potential, many theoretical models have been suggested to deal with V_{xc}, however, much of them are not mature. For example, the weighted density approximation (WDA) can't be used in the defect systems [22–24]. Here we adopt the LDA and GGA theoretical models which have been widely used in positron theoretical research area, and the parameterized expressions could be found in Refs. [25,26]. Ω is the volume of the unit cell, Z_α and $\rho(\boldsymbol{r}')$ represent the number of valence electron and the valence electron density of the atom respectively. According to equations (2)(5), the positron wavefunction and energy band can be obtained. A fully thermalized positron is assumed to be, in good approximation, at the bottom of the positron band with n = 1 and k = 0. After obtaining the wavefunction, almost all of the positron related parameters such as positron lifetime, effective mass et al. can be calculated. Details of the calculation formulas could be found in Refs. [6,24,27–29].

The most remarkable thing is that in positron chemical potential calculation, unlike the LMTO-ASA framework, there is a so-called pseudocore correction in the NCPP method. That is to say, the positron affinity $A_+ = \mu_- + \mu_+ = E_v + E_0 + \alpha$, where E_v is the top of electron valence band, E_0 is the ground state energy of the positron and α is just the pseudocore correction [8,30] which corrects the pseudo nature of the electron ion-core potential.

3. Results and discussion

The high frequency dielectric constants ε_∞ for C, Si and Ge are set to 5.62, 11.90 and 16.00, respectively [13]. Finally, the optimized lattice constants are 3.579 Å for C, 5.478 Å for Si and 5.783 Å for Ge, these parameters are specified in Table 1, and are all needed for calculating the positron levels. Work function is a surface related physical quantity, the same solid material with different crystal surface has a different work function. So, three surfaces [1 0 0], [1 1 0] and [1 1 1] have been used for calculating the electron work functions (Table 1).

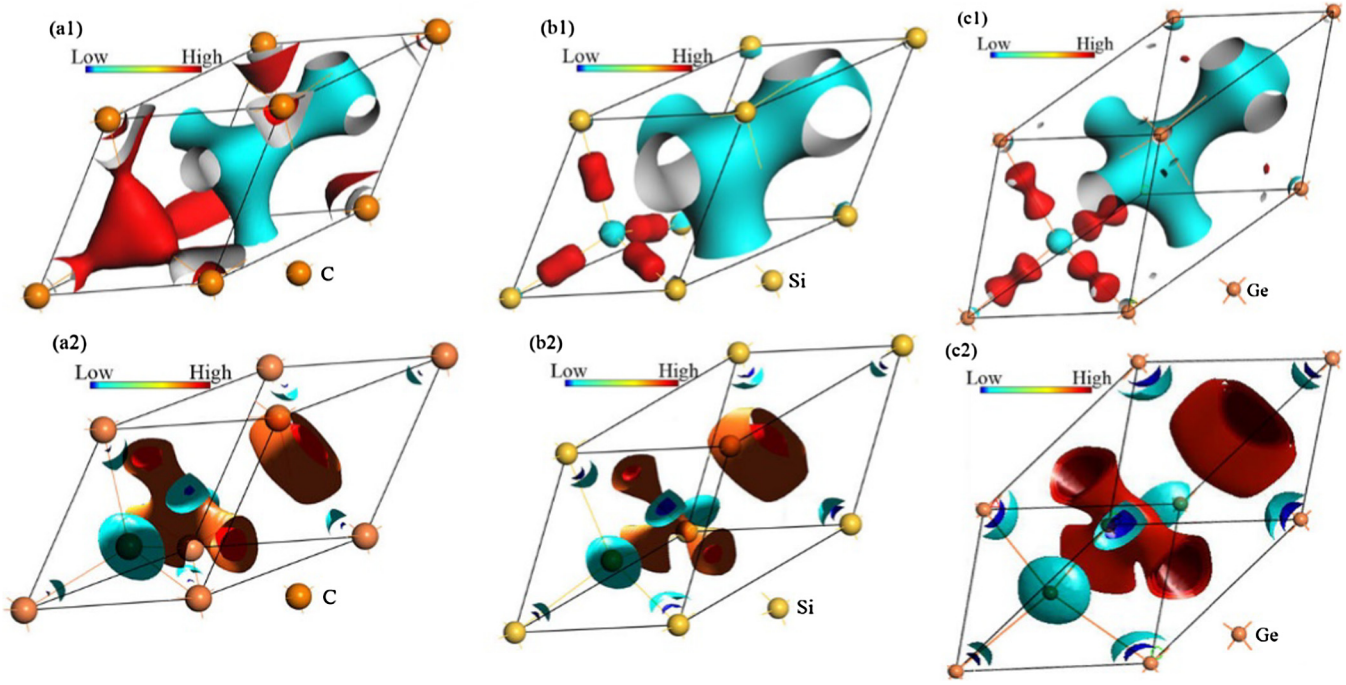

Fig. 3. The electron and positron density distribution isosurfaces of C, Si and Ge. (a1), (b1) and (c1) show the electronic isosurfaces and (a2) to (c2) display the positronic isosurfaces. The colorbars represent the low density to the high density color region. (For interpretation of the references to color in this figure legend, the reader is referred to the web version of this article.)

It can be seen that the electron work functions in the elemental semiconductors agree well with the experimental results in the Refs. [31,32], and this displays that here the NCPP can be used to predict the parameter at least for these simple solids. The distributions of thermalized positron densities along the ⟨1 1 1⟩ direction for C, Si and Ge are shown in Fig. 1. The atom positions are plotted, it is clear that the exclusion of the positron from the ionic cores. The dotted lines and solid lines express that the positron-electron EC potential are deal within the LDA and GGA schemes respectively. They have only a little difference and almost superposition with each other, so that readers may not catch sight of the dotted lines. This superposition is due to the fundamental principles of LDA and GGA, and results in only a little difference in positron lifetime, energy band and some other positron related parameters.

Aourag et al. have researched the positron level of C [33] within the empirical nonlocal pseudopotential method. The positron density distribution of C in this paper agrees well with their result which is shown in their Fig. 7. It is noteworthy that in order to have an optimal display, they added a constant to the positron density.

Panda et al. have used a pseudopotential method to study the positron level in Si [34]. In their paper, the positron-ion interaction potential was also calculated in the frozen-core approximation, but without point-core approximation, and the positron-electron EC potential was handled only within LDA scheme. They give a positron wave function along ⟨1 1 1⟩ direction with and without the EC potential in Fig. 2 in their paper. The square of the wave function is the probability density, and then multiply a normalized coefficient is just the density. It is apparent that there are two peaks between 4.5 a.u. and 16.0 a.u., they are located at about 8.75 a.u. and 13.25 a.u., this characteristic is similar to our result as is displayed in Fig. 1(b). However, Panda et al. given almost the same value of the two peaks. Here, the peak value at position 13.25 a.u. is obvious larger than the peak value at 8.75 a.u., this is not due to the point-core approximation effect in our scheme, but attribute to the electron density distribution. That is to say, positron wavefunction or to say positron density is sensitive to the accuracy of the valence charge density, this statement is different from Panda et al. [34]. In order to confirm our conclusion further, the free-atom superposition (ATSUP) method which was first proposed by Puska et al. [35] is also used to compute the positron density and the result is shown in Fig. 2. In order to have the comparability, the positron-electron EC potential is handled within LDA scheme both in the ATSUP and NCPP methods. Obviously, the positron densities have distinguished discrepancy in the interval and the bonding zones. Hence, not the positron wavefunction but the lifetime is not sensitive to the accuracy of the valence charge density.

Bouarissa et al. have studied the behavior of the positron in Ge by using the empirical pseudopotential method (EPM) coupled with the independent particle approximation [36]. In their paper, due to flat feature in the interstitial region, they didn't considered the positron- electron EC potential, and so the results are relatively coarse.

Due to the repulsion effect, the positron densities reduce to a vanishing point at the vicinity of the ion cores as is clear seen in Figs. 1 and 2. In addition, the positron tends to be pushed out of the primitive cell containing a larger valence and a larger ion core as had been pointed by Soudini et al. [37]. 3D views of the electron and positron density isosurfaces of C, Si and Ge in Fig. 3 could give a much more direct impression. Besides, the sp^3 electron orbital hybridization covalent bond could be seen intuitively, and the positron is inclined to stay in the tetragonal site than in the hexagonal site because of much more repulsion of ion core at the hexagonal site.

The positron energy bands of C, Si and Ge are shown in Fig. 4. The positron band structures in the figure with and without the positron-electron EC potential are plotted using solid and dashed lines respectively in order to resolve the difference. The bands of the three hosts are lined with their lowest energies set to zero. The lowest positron level is the most important level compared to other levels due to that the thermalized positron locates at this position. Generally, the lowest level is rather near the vacuum level, and the positron work function would be positive if the level is lower than the vacuum level, under this circumstance, the mate-

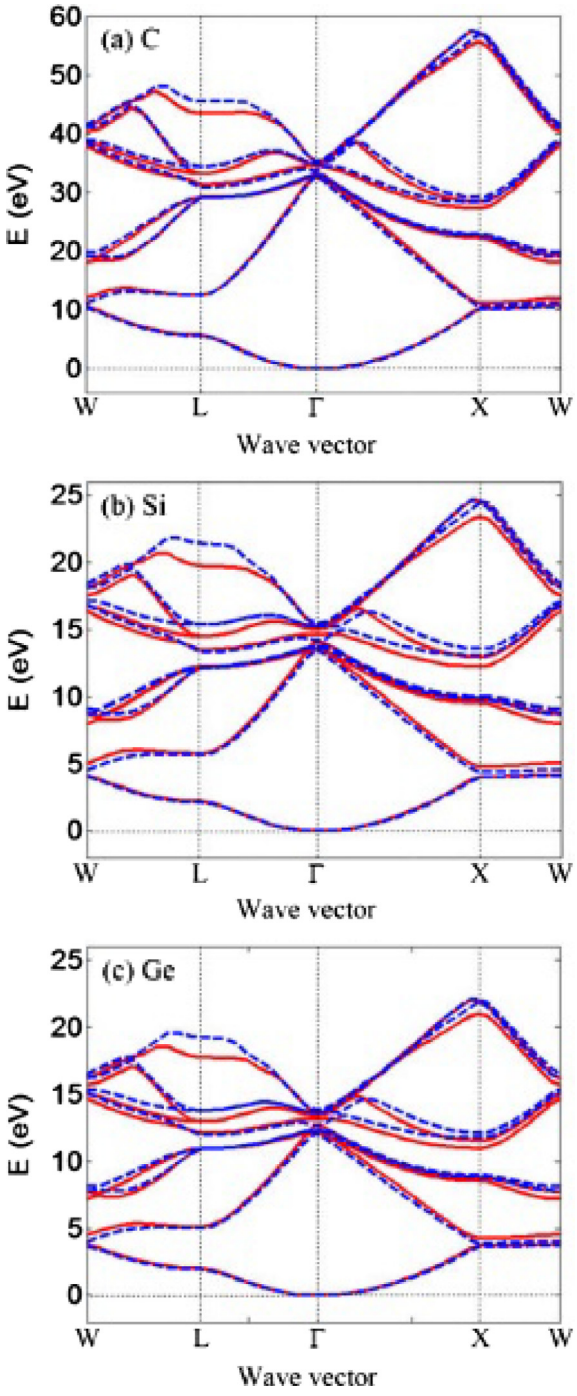

Fig. 4. The positron band structures of (a) C, (b) Si and (c) Ge, along the principal symmetry directions, the solid and dashed lines represent the results with and without the positron-electron EC potential respectively.

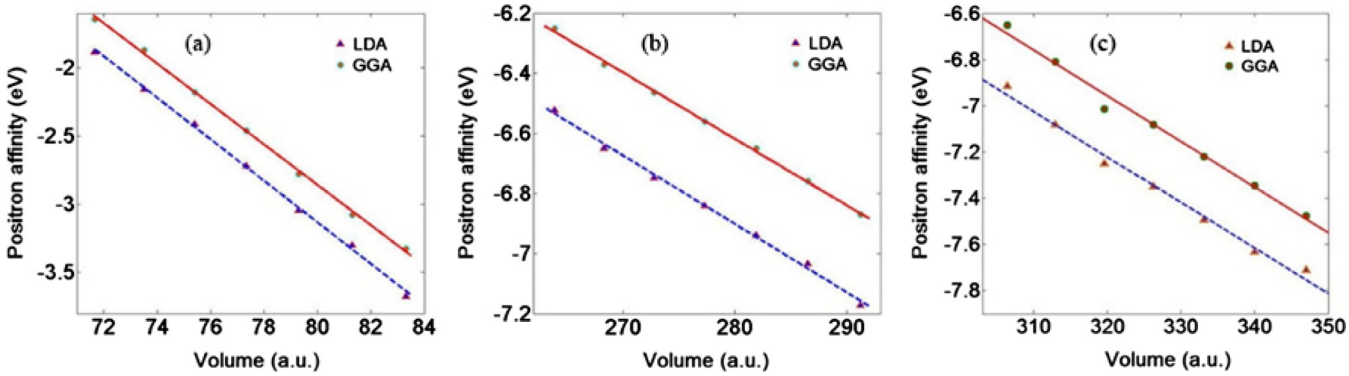

Fig. 5. The positron affinities (eV) of (a) C, (b) Si and (c) Ge as functions of the primitive cell volumes. The triangle and round dots represent the theoretical results within LDA and GGA respectively. The dashed and solid lines are the corresponding fitting results.

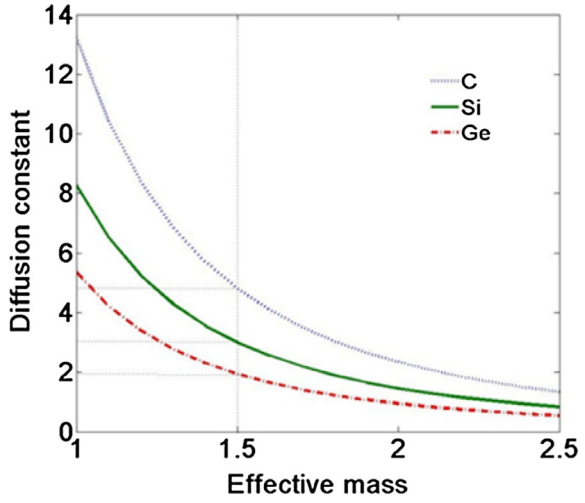

Fig. 6. Positron diffusion constant (unit: $cm^2\ s^{-1}$) as a function of the positron effective mass m^* (atomic unit) for C, Si and Ge. E_d^+ comes from GGA result and the absolute temperature T = 300 K.

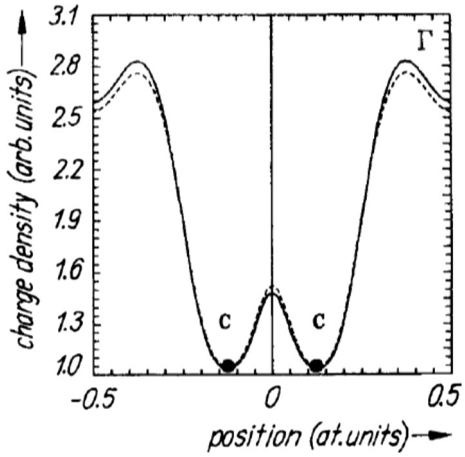

Fig. 7. The thermalized positron charge density along the ⟨1 1 1⟩ direction at normal pressure (solid lines) and under 10^{10} Pa (dashed lines).

rial may be used as a positron moderation. So, it has significant implications of the theoretical research on positron work function for finding the more appropriate moderation.

Because of some important distinctions with related exist research results, and there are more comparable data of Si, the Si positronic band structure is first discussed here. According to Fig. 4(b), there is almost no energy gap between the first and the second band when the positron-electron EC potential is not considered. This character is consistent with Refs. [34,38]. Due to that Aourag et al. also without considered the positron- electron EC potential [38], their results are of course very rough. This had changed more or less later in the Panda's paper [34] where the EC potential was included.

On the whole, the change performances of the two lowest bands in Fig. 4(b) are similar with Fig. 3 in [38] and Fig. 1 in [34]. However, in the higher bands, there are some visible differences. For example, the third and fourth band in the Γ-X direction are almost in the degenerate state from Fig. 4(b). This is consistent with reference [34] but different from [38]. The reason is that, the EPM Aourag et al. had used is not precise enough to construct the valence charge density and hence the band structure they obtained is not very accurate. At the Γ point, there is a large gap between the second and third band in paper [34], however, Aourag et al. and us give an invisible energy gap. This feature mainly comes from the point-core approximation effect, because if we don't adopt this approximation, a large gap also exists in the same position. In addition, when the positron-electron EC potential is considered, a small energy gap appears between the first and second band in the X-W direction, it is different from the results in [34]. This is mainly due to the different EC potential we use, and the EC potential effect will produce systematically more influence in several lower band levels than higher band levels.

Similar conclusions also exist in host C and Ge [33,36]. However, it should be pointed that Fig. 2(a) and (b) in paper [36] may display oppositely for positron and electron band structures. That is to say, Fig. 2(a) in reference [36] is the positronic band and Fig. 2(b) should be the electronic band of Ge. The reason for this is simple: there should be no positronic energy gap between band 4 and band 5, and also there should be no electronic energy gap between band 1 and band 2.

Here, the so called "band-gap problem" is simply discussed. In the first-principle electronic structure calculations based on the standard Kohn-Sham (KS) scheme of density-functional theory (DFT), the band gaps in semiconductors or insulators are typically underestimated. In recent years, many approaches have been developed for dealing with this problems in different material systems. For example, in functionally graded phononic crystals, the explicit functionally graded model and the multilayer model, in conjunction with the transfer matrix method have been developed to treat the band gaps [39,40]. However, in usual crystals, there are mainly two theoretical schemes to solve this gap problem. One is the conventional DFT and the other is the many-body perturbation theory (MBPT) basing on the Green'n function. In DFT, the band gap E_g is the difference of KS eigenvalues plus a contribution which

Table 2
The specific values of positron band effective mass (atomic unit), positron affinity A_+ (eV), positron work function (eV), positron annihilation rate λ (ns^{-1}), and positron lifetime τ (ps). "NON" in the table represents that the positron-electron EC energy is not considered. λ is divided into two parts: the core electron (λ_c) and valence electron (λ_v) annihilation rare.

Host	EC	Band effective mass			A_+ (eV)	Positron work function (eV)			λ (ns^{-1})		τ (ps)
		[1 0 0]	[1 1 0]	[1 1 1]		⟨1 0 0⟩	⟨1 1 0⟩	⟨1 1 1⟩	λ_c	λ_v	
C	NON	1.10	1.11	1.13	–	–	–	–	–	–	–
	LDA	1.08	1.09	1.12	−2.72	−4.09	−2.24	−1.36	0.253	10.273	95
					−2.64 [8]	−3.83 [48]			0.145 [49]	11.88 [49]	83 [49]
	GGA	1.08	1.10	1.11	−2.46	−4.35	−2.50	−1.62	0.189	10.015	98
					−2.20 [8]				0.100 [18]	9.900 [18]	100 [18]
Si	NON	1.16	1.18	1.20	–	–	–	–	–	–	–
		1.360 [34]	1.362 [34]	1.361 [34]							
	LDA	1.12	1.15	1.18	−6.84	1.71	2.37	2.10	0.192	4.416	217
		1.326 [34]	1.333 [34]	1.332 [34]	−6.95 [9,32]	2.04 [32]		2.21 [32]	0.103 [49]	4.471 [49]	219 [49]
					−6.45 [8]						
	GGA	1.12	1.14	1.19	−6.56	1.43	2.09	1.82	0.131	4.520	215
					−5.91 [8]				0.125 [18]	4.505 [18]	216 [18]
Ge	NON	1.16	1.18	1.19	–	–	–	–	–	–	–
	LDA	1.11	1.14	1.17	−7.35	2.37	2.68	2.72	0.309	4.039	230
					−6.69 [9]	2.77 [50]		1.98 [32]	0.301 [49]	4.129 [49]	226 [49]
					−6.79 [32]			2.85 [50]			
	GGA	1.12	1.13	1.17	−7.08	2.10	2.41	2.45	0.263	4.047	232
									0.288 [18]	4.098 [18]	228 [18]

Table 3
The values of positron deformation potential E_d^+ (eV), elastic constant and diffusion constant (the total positron effective masses are all chosen as 1.5, absolute temperature T = 300 K) in the hosts.

Host	E_d^+ (eV)		c_{11} (Mbar)	c_{12} (Mbar)	c_{44} (Mbar)	$\langle c_{ii} \rangle$ (Mbar)	D_+ ($cm^2\ s^{-1}$)
	LDA	GGA					
C	−11.78	−11.59	10.34	1.15	5.52	11.26	4.81
	−11.92 [8]	−11.67 [8]	10.79 [51]	1.24 [51]	5.78 [51]	11.80 [51]	
Si	−6.24	−6.21	1.51	0.55	0.99	2.02	3.00
	−6.19 [9,32]	−5.91 [8]	1.66 [52]	0.64 [52]	0.80 [52]	1.95 [52]	3.05 [32]
	−6.39 [8]						2.3 [54]
Ge	−6.43	−6.45	1.03	0.34	0.73	1.41	1.94
	−6.62 [9,32]		1.29 [53]	0.48 [53]	0.67 [53]	1.56 [53]	2.13 [32]
							0.9–2.1 [54]

comes from the discontinuity Δ_{xc} of the EC potential at integer particle numbers. The DFT scheme usually carried out within the LDA/GGA, whose $\Delta_{xc} = 0$. This is one of the most important reason for the gap problem. The other significant point originates in the errors in the KS eigenvalues resulting from the approximate nature of the functional. In order to solve the two problems, many approximate models have been proposed. For example, the hybrid functional methods PBE0 (first proposed by Perdew et al. [41]), HSE06 (first proposed by Heyd et al., and then further improved by Krukau et al. in the year 2006 [42,43]) and so on. Although PBE0 and HSE06 yield realistic generalized KS gaps for typical semiconductors, but they can over or underestimate gaps of many other solids, for example, molecular crystals seem to need 1/ε of long range exact exchange. MBPT, especially the GW approximation have yielded electronic structures in good agreement with experiments in many materials [44]. Base on the GW, many methods such as the G_0W_0 [45], QSGW [46] et al. have been developed. However, the former G_0W_0 fails for compounds with d electrons, especially when d states hybridize with p states close to the Fermi energy and the later QSGW generates too large energy gap in many materials. In a word, great developments have been made. But these new approximation functions express a kind of great randomicity or empiricism, and they have limited application.

In positronic structure calculation, this gap problem becomes much more difficult. Because that there are positron-electron and positron-positron EC interactions. Both of them are not understood clearly so far. Therefore, few researchers give reliable systemic results of the positron energy gap and it needs for further study.

It is interesting that in these elemental semiconductors, the positron-electron EC interaction has not important role on the shape of the several lowest bands, especially on the first band. In other words, only the positron-electron coulomb interaction produces significant role on the positron band effective mass m_b^*, according to its definition (in atomic unit):

$$m_b^* = \left(\frac{\partial^2 E}{\partial k^2}\right)^{-1} \tag{6}$$

where E is the band level and k is the wave vector.

The specific values of band effective mass in C, Si and Ge are given in Table 2. From Table 2, it can be seen clearly that this mass is not sensitive of EC energy, and hence the results coming from LDA, GGA and without EC effect are very close to each other. Besides, the band effective mass is almost to being isotropic in these hosts, and becomes slightly heavier along the [1 1 1] direction due to that the positron experience more coulomb repulsive interaction. Due to the point-core approximation effect, this mass in Si is systematically a little lower than reference result. The total positron effective mass mainly contains two parts, one is just the m_b^* due to the periodic lattice, the other is so-called correlation effective mass coming from the screening electron cloud. When

m_b^* is obtained, the total effective mass could be easily calculated from the expression (3.1) in Ref. [34]. However, the strict determination of the total effective mass is a difficult many-body problem and different approximate approach would generate quite large different results [32,47]. Therefore, here we don't intend to give the specific values of this parameter for these semiconductors.

The calculated positron affinity, work function, positron annihilation rate and lifetime within LDA and GGA schemes are all given in Table 2. These results are consistent with related credible theoretical or experimental data in references. However, some of them are not found in existing papers as we have searched.

The deformation potential theory is usually adopted to research the positron-phonon interaction which plays a dominant role in the positron diffusion stage [26]. In the theory, the coupling strength is determined by the deformation potential E_d^+. For a positron in a solid, it is the volume derivatives of positron affinity:

$$E_d^+ = \Omega \frac{\partial A_+}{\partial \Omega} \tag{7}$$

In practical calculation, the volume derivatives of the positron affinity is determined by performing band structure calculations for several slightly different lattice constants. Fig. 5 shows the A_+as a function of volume around the equilibrium structure in C, Si and Ge, and Table 3 gives the values of E_d^+ for all the hosts. At last, the positron diffusion constant within the deformation potential theory scheme is given by:

$$D_+ = \left(\frac{8\pi}{9}\right)^{1/2} \cdot \frac{\hbar^4 \cdot \langle c_{ii} \rangle}{m^{*\frac{5}{2}} \cdot (k_B T)^{1/2} \cdot E_d^{+2}} \tag{8}$$

where m^* is the positron effective mass, T is the absolute temperature and $\langle c_{ii} \rangle$ is the elastic constant associated with longitudinal waves. For simplicity, here we approximate it for the [1 1 0] plane by:

$$\langle c_{ii} \rangle = 0.5(c_{11} + c_{12} + 2c_{44}) \tag{9}$$

According to Eq. (8), it could be easily seen that D_+ is sensitive to the physical quantity m^*. Because of the difficulty for strict computing the total effective mass, the specific values of positron diffusion constants in Table 3 are given with all of the m^* are chosen as 1.5 (this chosen is reasonable [32]), and $D_+$are displayed as a function of m^* as shown in Fig. 6.

4. Conclusions

The positron level and related positron parameters such as positron affinity, work function, deformation potential, effective mass and so on are systematic researched in diamond structure elemental semiconductors using the first-principle NCPP method. Only the GGA scheme is adopted in the electronic band structure calculations, while in the positronic computations, both the LDA and GGA are used. The so- called nonlinear core correction is included and the core electrons are deal within the frozen-core approximation. The point-core approximation is used to model the ionic potential. It is found that although the positron lifetime is not sensitive to the electron density distribution, the positron wavefunction or to say positrton density has an opposite behavior, especially in the interstitial and bonding sites.

The positron-electron EC energy has not very important role in shapes of the several low energy bands especially in the first band, this gives rise to that the EC energy doesn't generate a significant influence on the effective band mass. However, it will produce a little energy gap in the X-W direction between the band 1 and band 2.

Through the systematic research of the positron related parameters in elemental semiconductors, it can be seen that point-core approximation could provide reliable theoretical result within in NCPP framework. However, because of the loss of the exact positron-ion potential, it could not give a precise positron effective band mass. The band mass is the key component of the total positron effective mass, and the diffusion coefficient is sensitive to this total effective mass. Therefore, the approximation model could not predict the positron diffusion coefficient accurately.

References

[1] Peter J. Schultz, K.G. Lynn, Rev. Mod. Phys. 60 (1988) 701.
[2] R. Krause-Rehberg, H.S. Leipner, Positron Annihilation in Semiconductors: Defect Studies, Springer, Berlin, 1999.
[3] Y. Nagai, T. Chiba, Z. Tang, T. Akahane, T. Kanai, M. Hasegawa, M. Takenaka, E. Kuramoto, Phys. Rev. Lett. 87 (2001) 176402.
[4] H. Haghighi, J.H. Kaiser, S. Rayner, R.N. West, J.Z. Liu, R. Shelton, R.H. Howell, F. Solal, M.J. Fluss, Phys. Rev. Lett. 67 (1991) 382.
[5] B. Barbiellini, M.J. Puska, T. Korhonen, A. Harju, T. Torsti, R.M. Nieminen, Phys. Rev. B 53 (1996) 16201.
[6] M.J. Puska, R.M. Nieminen, Rev. Mod. Phys. 66 (1994) 841.
[7] G.R. Brandes, A.P. Mills Jr., Phys. Rev. B 58 (1998) 4952.
[8] B.K. Panda, G. Brauer, W. Skorupa, J. Kuriplach, Phys. Rev. B 61 (2000) 15848.
[9] M.J. Puska, P. Lanki, R.M. Nieminen, J. Phys.: Condens. Matter 1 (1989) 6081.
[10] J. Kuriplach, M. Sob, G. Brauer, W. Anwand, E.-M. Nicht, P.G. Coleman, N. Wagner, Phys. Rev. B 59 (1999) 1948.
[11] M.J. Puska, R.M. Nieminen, Phys. Rev. B 46 (1992) 1278.
[12] G. Brauer, W. Anwand, E.-M. Nicht, J. Kuriplach, M. Sob, N. Wagner, P.G. Coleman, M.J. Puska, T. Korhonen, Phys. Rev. B 54 (1996) 2512.
[13] J.M. Campillo Robles, E. Ogando, F. Plazaola, J. Phys.: Condens. Matter 19 (2007) 176222.
[14] J.P. Perdew, K. Burke, Phys. Rev. Lett. 77 (1996) 3865.
[15] Z. Wu, R.E. Cohen, Phys. Rev. B 73 (2006) 235116.
[16] J. Neugebauer, M. Scheffler, Phys. Rev. B 46 (1992) 16067.
[17] S.G. Louie, S. Froyen, M.L. Cohen, Phys. Rev. B 26 (1982) 1738.
[18] B.K. Panda, W. LiMing, S. Fung, C.D. Beling, Phys. Rev. B 56 (1997) 7356.
[19] Z. Tang, M. Hasegawa, T. Chiba, M. Saito, H. Sumiya, Y. Kawazoe, S. Yamaguchi, Phys. Rev. B 57 (1998) 12219.
[20] N. Bouarissa, J. Phys. Chem. Solids 67 (2006) 1440.
[21] Y. Al-Douri, J. Appl. Phys. 93 (2003) 9730.
[22] A. Rubaszek, Z. Szotek, W.M. Temmerman, Phys. Rev. B 58 (1998) 11285.
[23] A. Rubaszek, Z. Szotek, W.M. Temmerman, Phys. Rev. B 61 (2000) 10100.
[24] F. Tuomisto, I. Makkonen, Rev. Mod. Phys. 85 (2013) 1583.
[25] E. Boronski, R.M. Nieminen, Phys. Rev. B 34 (1986) 3820.
[26] J. Kuriplach, B. Barbiellini, Phys. Rev. B 89 (2014) 155111.
[27] B.K. Panda, S. Fung, C.D. Beling, Phys. Rev. B 53 (1996) 1251.
[28] M.A. van Huis, A. van Veen, H. Schut, C.V. Falub, S.W.H. Eijt, P.E. Mijnarends, J. Kuriplach, Phys. Rev. B 65 (2002) 085416.
[29] M.J. Puska, J. Phys.: Condens. Matter 3 (1991) 3455.
[30] M.C. Payne, M.P. Teter, D.C. Allan, T.A. Arias, J.D. Joannopoulos, Rev. Mod. Phys. 64 (1992) 1045.
[31] J.B. Cui, J. Ristein, L. Ley, Phys. Rev. B 60 (1999) 16135.
[32] O.V. Boev, M.J. Puska, R.M. Nieminen, Phys. Rev. B 36 (1987) 7786.
[33] H. Aourag, S. Ait Abderrahmane, Na. Amrane, N. Amrane, N. Bouarissa, Phys. Stat. Sol. (b) 189 (1995) 417.
[34] B.K. Panda, Y.Y. Shan, S. Fung, C.D. Beling, Phys. Rev. B 52 (1995) 5690.
[35] M.J. Puska, R.M. Nieminen, J. Phys. F: Met. Phys. 13 (1983) 333.
[36] N. Bouarissa, B. Abbar, J.P. Dufour, N. Amrane, H. Aourag, Mater. Chem. Phys. 44 (1996) 267.
[37] B. Soudini, H. Aourag, N. Amrane, M. Gamoudi, B. Khelifa, Comput. Mater. Sci. 1 (1993) 373.
[38] H. Aourag, A. Belaidi, T. Kobayasi, R.N. West, B. Khelifa, Phys. Stat. Sol. (b) 156 (1989) 497.
[39] M.V. Golub, S.I. Fomenko, T.Q. Bui, Ch. Zhang, Y.-S. Wang, Int. J. Solids Struct. 49 (2012) 344.
[40] S.I. Fomenko, M.V. Golub, Ch. Zhang, T.Q. Bui, Y.-S. Wang, Int. J. Solids Struct. 51 (2014) 2491.
[41] J.P. Perdew, M. Ernzerhof, K. Burke, J. Chem. Phys. 105 (1996) 9982.
[42] J. Heyd, G.E. Scuseria, M. Ernzerhof, J. Chem. Phys. 118 (2003) 8207.
[43] A.V. Krukau, O.A. Vydrov, A.F. Izmaylov, G.E. Scuseria, J. Chem. Phys. 125 (2006) 224106.
[44] G. Onida, L. Reining, A. Rubio, Rev. Mod. Phys. 74 (2002) 601.
[45] W.G. Aulbur, L. Jonsson, J.W. Wilkins, Solid State Phys. 54 (1999) 1.
[46] S.V. Faleev, M. van Schilfgaarde, T. Kotani, Phys. Rev. Lett. 93 (2004) 126406.
[47] T. Hyodo, T. McMullen, A.T. Stewart, Phys. Rev. B 33 (1986) 3050.
[48] G.R. Brandes, A.P. Mills, D.M. Zuckerman, Mater. Sci. Forum 105–110 (1992) 1363.
[49] M.J. Puska, S. Makinen, M. Manninen, R.M. Nieminen, Phys. Rev. B 39 (1989) 7666.
[50] N.G. Fazleev, J.L. Fry, A.H. Weiss, Mater. Sci. Forum 255–257 (1997) 145.
[51] H.J. McSkimin, P. Andreatch Jr., P. Glynn, J. Appl. Phys. 43 (1972) 985.
[52] H.J. McSkimin, P. Andreatch Jr., J. Appl. Phys. 35 (1964) 2161.
[53] H.J. McSkimin, P. Andreatch Jr., J. Appl. Phys. 34 (1963) 651.
[54] E. Soininen, J. Makinen, D. Beyer, P. Hautojarvi, Phys. Rev. B 46 (1992) 13104.